Stability of periodic progressive gravity wave solutions of the Whitham equation in the presence of vorticity

C. Kharif[a], M. Abid[a], J. D. Carter[b], H. Kalisch[c]

[a] *Aix Marseille Université, CNRS, Centrale Marseille, IRPHE UMR 7342, F-13384, Marseille, France*
[b] *Mathematics Department, Seattle University, USA*
[c] *Department of Mathematics, University of Bergen, Norway*

Abstract

The modulational instability of two-dimensional nonlinear traveling-wave solutions of the Whitham equation in the presence of constant vorticity is considered. It is shown that vorticity has a significant effect on the growth rate of the perturbations and on the range of unstable wavenumbers. Waves with kh greater than a critical value, where k is the wavenumber of the solution and h is the fluid depth, are modulationally unstable. This critical value decreases as the vorticity increases.

Additionally, it is found that waves with large enough amplitude are always unstable, regardless of wavelength, fluid depth, and strength of vorticity. Furthermore, these new results are in qualitative agreement with those obtained by considering fully nonlinear solutions of the water-wave equations.

Keywords: Whitham equation; modulational instability; vorticity

1. Introduction

It is well known that small-amplitude, two-dimensional, periodic wave trains are stable with respect to the modulational instability when the dispersive parameter kh, where k is the wavenumber and h is the mean fluid depth, is less than the critical value 1.363. Nevertheless, McLean [1] found that Stokes waves are modulationally unstable when $kh = 1$ and $ak = 0.29$, where a is the wave amplitude. We can conjecture that strongly nonlinear

*Corresponding author: kharif@irphe.univ-mrs.fr

uniform wave trains are modulationally unstable with respect to infinitesimal perturbations in shallow water. To extend the results of McLean [1] to shallower water, Francius and Kharif [2] investigated instabilities of periodic gravity waves in shallow water using the fully nonlinear potential Euler equations. For small values of ak, they found that the dominant instabilities are quasi-two-dimensional whereas for moderate and large steepness, the dominant instabilities are three-dimensional.

Whitham [3] proposed an extension of the KdV equation by using the full linear dispersion instead of its third-order truncated expression. Consequently, the Whitham equation presents an improvement over the KdV equation for short waves. In fact, Carter [4] showed that the Whitham equation provides a more accurate model for experimental initial waves of depression than does the KdV equation. Similarly, Moldabayev, Kalisch and Dutykh [5] showed that solutions of the Whitham equation stay close to solutions of the Euler equations, and Klein et al. [6] gave a mathematical proof that solutions of the Euler equations are well approximated by solutions of the Whitham equation on small to intermediate time scales.

Ehrnström and Kalisch [7, 8] proved rigorously that the Whitham equation admits small and large amplitude, periodic traveling-wave solutions and numerically computed traveling-wave solutions with a variety of amplitudes including those close to the highest wave. Later on, Kharif and Abid [9] computed steadily propagating periodic waves in the presence of constant vorticity. The method of computing these solutions was developed by Ehrnström and Kalisch [8] and is also found in Sanford *et al.* [10] and Kharif and Abid [9]. Sanford *et al.* [10] studied the Whitham equation and found that two-dimensional, periodic wave trains with $kh = 1$ are stable when the wave steepness, ak, is less than approximately 0.142 and are unstable when the wave steepness is larger than this threshold. To a certain extent, this result is surprising because the Whitham equation is valid for weakly nonlinear water waves. The latter authors numerically corroborated the stability analysis of Hur and Johnson [11] who found that small-amplitude waves with $kh < 1.145$ are stable and are unstable when $kh > 1.145$. Note that Benjamin and Feir [12] and Whitham [13] showed that Stokes waves are unstable with respect to long wavelength perturbations if $kh > 1.363$. Later on, Hur and Johnson [14] incorporated in the Whitham equation the effect of constant vorticity which modifies the threshold value of the dispersive parameter.

Following Whitham [3], Kharif *et al.* [15] and Kharif and Abid [9] proposed a new model derived from the Euler equations for fully nonlinear wa-

ter waves propagating on a vertically sheared current of constant vorticity in shallow water that satisfies the unidirectional linear dispersion relation. From this model they derived, within the framework of weakly nonlinear waves, a generalization of the Whitham equation which they named the vor-Whitham equation. At the same time, Hur [16] and Bjørnestad and Kalisch [17] derived shallow water wave equations in the presence of constant vorticity.

In order to extend the previous studies of Sanford *et al.* [10] and Hur and Johnson [14], we consider the spectral stability of two-dimensional, periodic traveling-wave solutions of the Whitham equation in the presence of constant vorticity. Our study focuses on the modulational instability. The second aim is to show that the Whitham equation, which is an approximate equation that is easier to work with than the fully nonlinear water wave equations, may provide reliable stability results that are in qualitative agreement with those of the full equations.

In section 2, we present the vor-Whitham equation. In section 3, we describe how to compute the stationary solutions to this equation. Additionally, we present the stability of these solutions with respect to infinitesimal perturbations, the growth rates of instabilities, and the ranges of unstable Floquet parameters as functions of vorticity. Section 4 contains a conclusion of this work.

2. The vor-Whitham equation

We consider two-dimensional gravity waves that propagate on the surface of an inviscid, incompressible fluid with a shear current parallel to the direction of wave propagation that varies linearly in the vertical direction. We assume that the waves travel along the $x-$axis and that the $z-$axis is oriented upward with $z = 0$ representing the unperturbed free surface. In order to focus on the effects due to vorticity, we assume that the current velocity is zero at the free surface. In this situation, the current vorticity, Ω, is constant and the vor-Whitham equation is given by

$$\eta_t + c_1(\Omega)\eta\eta_x + K * \eta_x = 0, \tag{1}$$

where $\eta(x,t)$ represents the free surface displacement and t represents time. The coefficient of the nonlinear term is

$$c_1(\Omega) = \frac{3gh + h^2\Omega^2}{h\sqrt{4gh + h^2\Omega^2}},$$

where g is the gravitational constant of acceleration. The dispersive term is given by the convolution product, $K * \eta_x$, which is the inverse Fourier transform of the product of the Fourier transforms of $K(x)$ and $\eta_x(x,t)$. The integral kernel is

$$K(x) = \frac{1}{2\pi}\int_{-\infty}^{+\infty} c(k)e^{ikx}dk,$$

where the unidirectional dispersion of linear waves in the presence of vorticity is

$$c(k) = \frac{\Omega\tanh(kh)}{2k} + \sqrt{\frac{g\tanh(kh)}{k} + \frac{\Omega^2\tanh^2(kh)}{4k^2}}.$$

We consider traveling-wave solutions of the vor-Whitham equation of the form $\eta(x,t) = \bar{\eta}(x - c_0 t)$ for a given phase velocity c_0. Substituting this ansatz into equation (1) and integrating once leads to the equation that defines c and $\bar{\eta}$

$$-c_0\bar{\eta} + c_1(\Omega)\frac{\bar{\eta}^2}{2} + K * \bar{\eta} = B, \tag{2}$$

where B is the constant of integration. We choose B so that the solution $\bar{\eta}$ has zero mean.

3. Stability analysis

3.1. Steady waves

In the frame of reference moving with the traveling-wave solution, the vor-Whitham equation is given by

$$\eta_\tau - c_0\eta_X + c_1(\Omega)\eta\eta_X + K * \eta_X = 0, \tag{3}$$

where $X = x - c_0 t$ and $\tau = t$. In this frame of reference, the traveling-wave solution, $\bar{\eta}(X)$, is stationary (independent of τ) and satisfies equation (2). To compute these solutions, we use the numerical method of Ehrnström and Kalisch [7]. Details of the numerical method and its validation are found in Kharif and Abid [9]. However, herein we add a supplementary equation that fixes the wave amplitude when following solutions using c_0 as the continuation parameter.

In order to put the equations in dimensionless form, h and $\sqrt{h/g}$ are chosen as the reference length and reference time, respectively. This choice

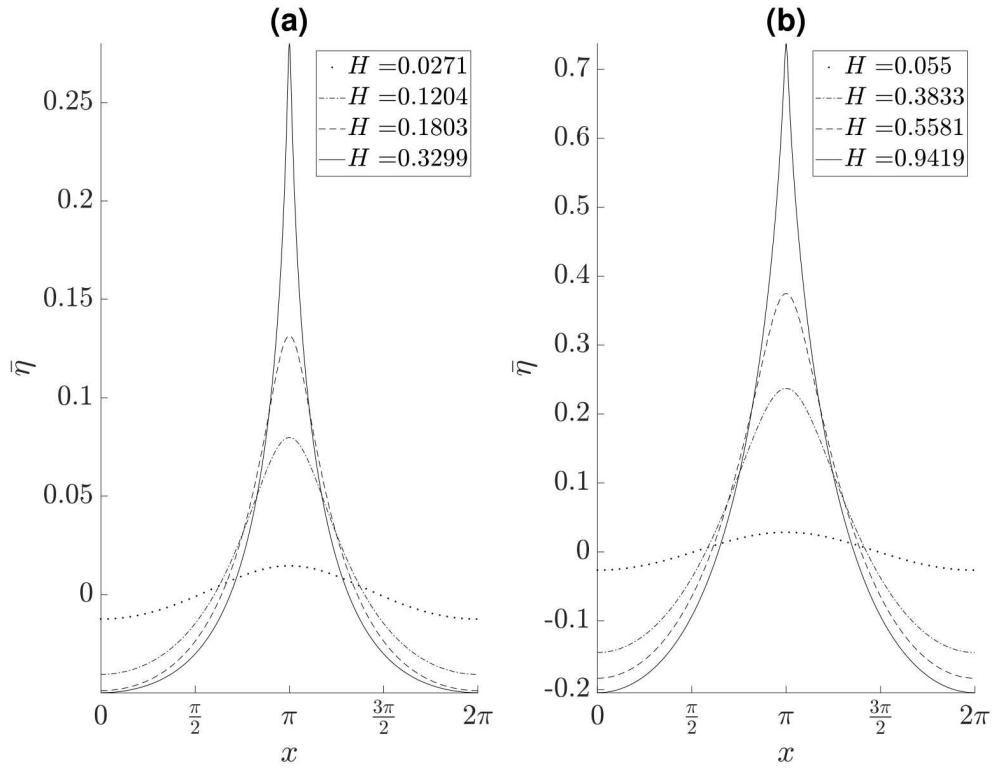

Figure 1: Plots of periodic traveling-wave solutions to the vor-Whitham equation with $L = 2\pi$, wave height, H (see captions), and (a) $\Omega = -1.0$, (b) $\Omega = 1.0$. Note that the vertical scales in the two plots are different.

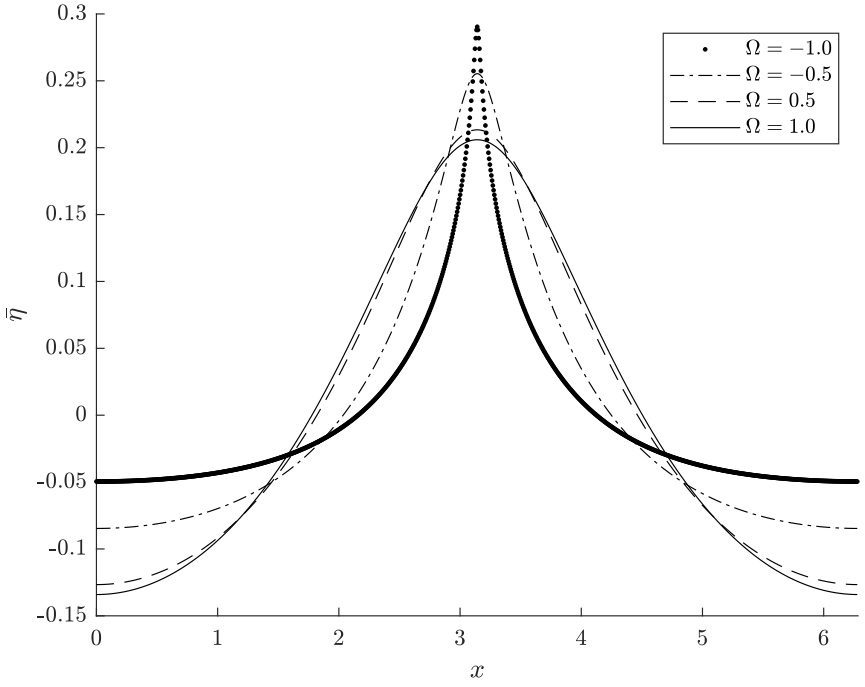

Figure 2: Plots of periodic traveling-wave solutions to the vor-Whitham equation with wave height, $H = 0.34$, $L = 2\pi$, and four different values of Ω.

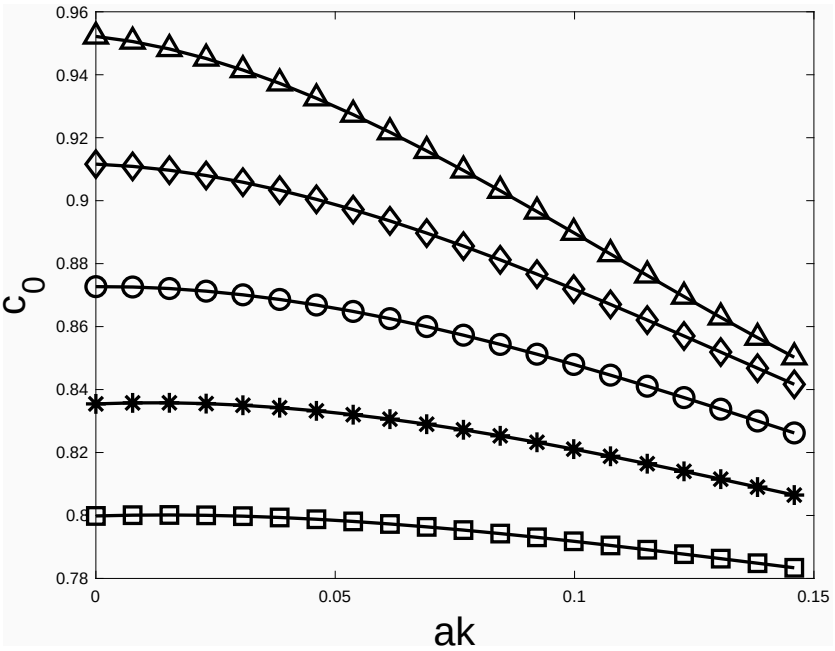

Figure 3: Phase velocity of the traveling-wave solutions as a function of the wave steepness for several values of the vorticity. $\Omega = 0\,(\circ), -0.1\,(*), 0.1\,(\diamond), -0.2\,(\square), 0.2\,(\triangle)$.

corresponds to setting $h = 1$ and $g = 1$. We consider 2π-periodic traveling-wave solutions to the vor-Whitham equation. Consequently, the wavenumber of these solutions is $k = 1$.

Figure 1 shows profiles of traveling-wave solutions to the vor-Whitham equation for two values of Ω and four values of the wave steepness. These plots, along with others left out for brevity, demonstrate that: (i) solutions corresponding to different values of Ω and L are qualitatively similar, (ii) for solutions with a given period and vorticity, increasing wave speed increases wave height and steepness, and (iii) there appears to be a solution of maximal height for all wave periods and values of vorticity.

Figure 2 shows profiles of traveling-wave solutions to the vor-Whitham equation with wave height 0.34 and four values of Ω. These plots, along with others left out for brevity, demonstrate that: (i) for solutions with a given period and wave height, increasing vorticity causes the width of the solution to increase and (ii) for solutions with a given period and wave height, increasing vorticity causes both the minima and maxima of $\bar{\eta}$ to decrease.

Figure 3 displays the phase velocity as a function of wave steepness for five values of the vorticity. These plots show that the phase velocity decreases as the wave steepness increases. For fixed values of the wave steepness, c_0 increases as Ω increases. This feature was observed by Kharif and Abid [9] within the framework of a fully nonlinear, generalized vor-Whitham equation, whereas the profiles shown in figure 1 are weakly nonlinear.

3.2. Stability of steady solutions

In order to study the stability of these solutions with respect to infinitesimal perturbations, let

$$\eta(X,\tau) = \bar{\eta}(X) + \eta'(X,\tau), \qquad |\eta'| \ll |\bar{\eta}|, \tag{4}$$

where $\bar{\eta}(X)$ and $\eta'(X,\tau)$ correspond to the 2π-periodic unperturbed steady solution and infinitesimal square integrable disturbance, respectively. Substituting equation (4) into equation (3) and linearizing gives the following equation which governs the (linear) evolution of the perturbations

$$\eta'_\tau - c_0\eta'_X + c_1(\Omega)(\bar{\eta}\eta'_X + \bar{\eta}_X\eta') + K * \eta'_X = 0. \tag{5}$$

The Fourier-Floquet-Hill method of Deconinck and Kutz [18], Johnson [19] establishes that all bounded solutions of this problem have the form

$$\eta'(X,\tau) = \exp(\lambda\tau)\exp(ipX)\sum_{j=-\infty}^{+\infty} a_j \exp(ijX), \tag{6}$$

where p is a real number known as the Floquet parameter. Substituting equation (6) into equation (5) gives

$$\sum_{-\infty}^{+\infty}(c_0-c_1(\Omega)\bar{\eta}-c_{p+j})i(p+j)a_j\exp(ijX)-c_1(\Omega)\bar{\eta}_X\sum_{-\infty}^{+\infty}a_j\exp(ijX)=\lambda\sum_{-\infty}^{+\infty}a_j\exp(ijX), \tag{7}$$

where

$$c_{p+j}=\frac{\Omega\tanh(p+j)}{2(p+j)}+\sqrt{\frac{\tanh(p+j)}{(2(p+j)}+\frac{\Omega^2\tanh^2(p+j)}{4(p+j)^2}}.$$

Equation (7) is transformed into a generalized eigenvalue problem for λ, which after truncation at M Fourier modes can be written as follows

$$\mathbf{Au}=\lambda\mathbf{Bu}, \tag{8}$$

where $\mathbf{u}=(a_{-M},...,a_0,...,a_M)^T$ is the corresponding eigenvector. The $2M+1$ unknown coefficients $(a_{-M},...,a_0,...,a_M)$ are chosen to satisfy (7) at $2M+1$ collocation points equally distributed along one period of the unperturbed solution. We used $M=100$ and checked that the results are the same within seven significant figures when doubling this value. The complex-valued matrices $\mathbf{A}$ and $\mathbf{B}$ depend on the unperturbed wave, $\bar{\eta}$, the vorticity, Ω, and the Floquet parameter, p. Once the unperturbed traveling-wave solution has been computed and p fixed, the generalized eigenvalue problem (8) is solved by using a standard numerical eigenvalue solver.

The eigenvalue spectrum corresponding to the flat surface ($\bar{\eta}=0$) is

$$\lambda_j=i(p+j)c_0-i(p+j)c_{p+j},$$

where the phase velocity of the flat surface is

$$c_0=\Omega\tanh(1)/2+\sqrt{\tanh(1)+\Omega^2\tanh^2(1)/4}.$$

All of these eigenvalues lie on the imaginary axis. Therefore, the flat surface is spectrally stable. The corresponding eigenfunctions are $\eta_j'=a_j\exp(\lambda_j\tau)\exp(i(p+j)X)$ which represent infinitesimal waves of frequency $(p+j)c_0-(p+j)c_{p+j}$ in the moving frame of reference and wavenumber $p+j$.

As the amplitude of the unperturbed wave increases from zero, the eigenvalues move on the imaginary axis and eigenvalue collisions occur. A necessary, but not sufficient, condition for instability is the collision of eigenvalues. The collision of eigenvalues can be expressed as

$$\lambda_{j_1}(p) = \lambda_{j_2}(p), \tag{9}$$

where the corresponding wavenumbers are $k_1 = p + j_1$ and $k_2 = p + j_2$. McLean *et al.* [20] divided the solutions of (9) into two classes. Depending upon whether $j_1 - j_2$ is even or odd, instabilities belong to class I or class II, respectively. Without loss of generality, it is convenient to assume that $j_2 = -j_1$ for class I and $j_2 = -j_1 - 1$ for class II. Herein, we focus only on class I with $j_1 = 1$ which correspond to instability of modulational type. These assumptions allow equation (9) to be rewritten as

$$2c_0 = (1 + p)c_{1+p} + (1 - p)c_{1-p}, \tag{10}$$

with

$$2k_0 = k_1 + k_2, \tag{11}$$

where $k_0 = 1$, $k_1 = 1+p$ and $k_2 = 1-p$. The subharmonic and superharmonic sidebands correspond to k_2 and k_1, respectively. Equations (10) and (11) can be interpreted as the resonance of two infinitesimal waves (sidebands) with the basic wave, i.e. a resonant four-wave interaction.

3.3. Numerical results

As a check on our numerical approach, we considered the case of Sanford *et al.* [10] corresponding to the 2π-periodic solution shown in their figure 3(b) with $c_0 = 0.8002$. We found that the maximum rate of growth is 0.000356 and the frequency is 0.00751 corresponding to $p = \pm 0.04056$. These values obtained with $\Omega = 0$ are very close to those of Sanford *et al.* [10]. Note that we used their transformation $\eta \to 3\eta/4$ in order to ensure that our Whitham equation and solution were the same as theirs. Additionally, Sanford *et al.* [10] showed that the traveling-wave solutions are stable to the modulational instability if their wave steepness is less than approximately 0.142 which corresponds to $ak \approx 0.19$ in our scaling (see table 1).

We carried out the stability computations for solutions with steepness $ak = 0.05$ and $ak = 0.10$ for a range of Ω values. We found that they are both stable with and without vorticity. Consequently, we decided to examine

ak	p	$\mathcal{R}e(\lambda)_{max}$
0.20	0.101	1.67×10^{-3}
0.19	0.005	0.811×10^{-4}
0.18	0.003	4.19×10^{-5}
0.17		$\mathcal{O}(10^{-11})$
0.15		$\mathcal{O}(10^{-11})$
0.10		$\mathcal{O}(10^{-12})$
0.05		$\mathcal{O}(10^{-12})$

Table 1: Growth rate of the most unstable perturbation as a function of the basic wave steepness without vorticity.

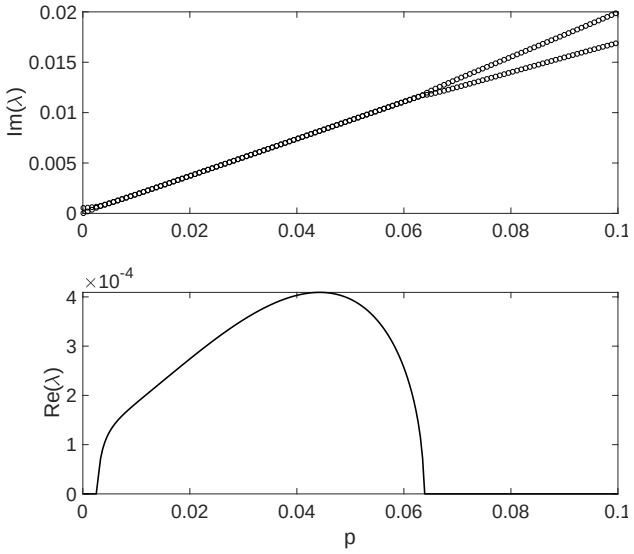

Figure 4: Radian frequency (top) and rate of growth (bottom) of the normal mode perturbation against its wavenumber for $\Omega = 0$ and $ak = 0.20$

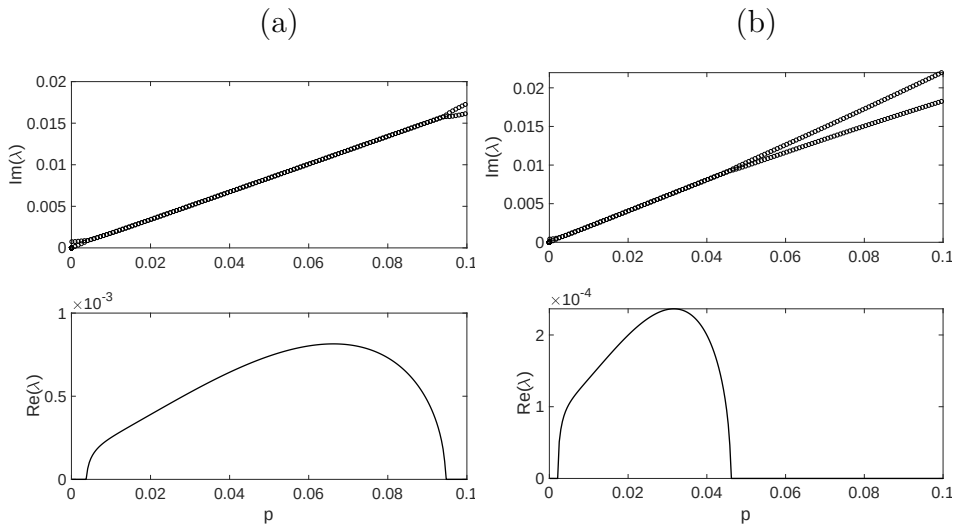

Figure 5: Radian frequency (top) and rate of growth (bottom) of the normal mode perturbation against its wavenumber for $ak = 0.20$ and (a) $\Omega = -0.1$ (b) $\Omega = 0.1$.

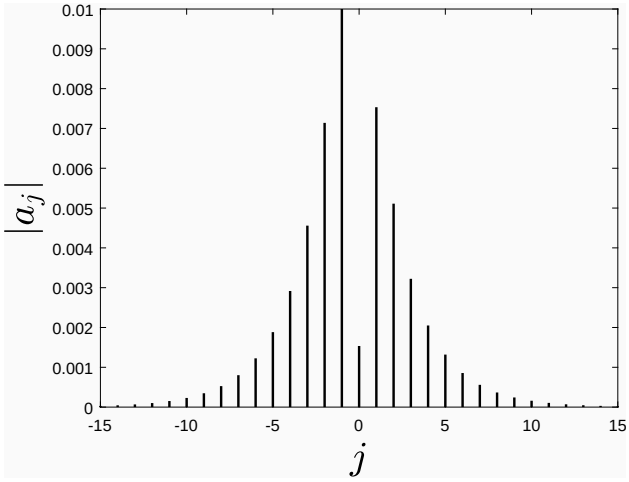

Figure 6: Magnitude of the coefficient a_j of the most unstable normal mode corresponding to $\Omega = 0.1$ and $ak = 0.20$.

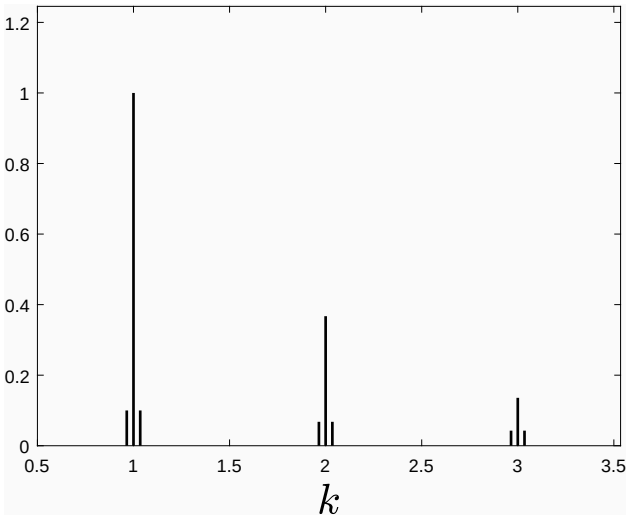

Figure 7: Amplitude spectrum of the unperturbed wave of wave steepness $ak = 0.20$ perturbed by its most unstable normal mode for $\Omega = 0.1$. The amplitudes of the Fourier components have been normalized by the amplitude of the fundamental mode $k = 1$ of the unperturbed wave.

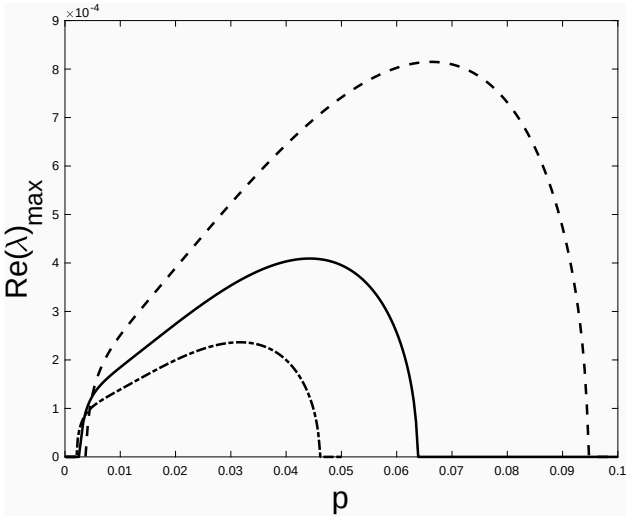

Figure 8: Maximum growth rate against the wavenumber for $\Omega = 0$ (solid line), $\Omega = -0.1$ (dashed line), $\Omega = 0.1$ (dot-dashed line) and $ak = 0.20$

the stability of traveling-wave solutions of wave steepness $ak = 0.20$, a value larger than the critical value in the $\Omega = 0$ case.

Figures 4 and 5 contain plots of $\mathrm{Im}(\lambda)$ and $\mathrm{Re}(\lambda)$ versus p, the wavenumber of the normal mode perturbation for three values of the vorticity and $ak = 0.20$. The upper plots in these figures show the collisions of two purely imaginary in the vicinity of the origin. These collisions give rise to instabilities corresponding to intervals of instability shown in the lower plots. These plots show that for a fixed value of the wave steepness both the rate of growth and the size of the interval of instability increase as Ω decreases. These plots also show that there are no instabilities with the same wavenumber as the unperturbed solution (i.e. $p = 0$) for any of the values of vorticity we examined.

Figure 6 shows the magnitudes of the coefficients a_j for the most unstable perturbation corresponding to $\Omega = 0.10$ and $ak = 0.20$. The two dominant components, $j = -1$ and $j = 1$, correspond to subharmonic and superharmonic sidebands typical of modulational instability. Note that the wavenumbers of the subharmonic and superharmonic sidebands are $1 - p$ and $1 + p$, respectively. Figure 7 shows the amplitude spectrum of the unperturbed wave of wave steepness $ak = 0.20$ perturbed by its most unstable normal mode. The physical perturbation corresponds to the real part of the perturbation given in equation (6). The amplitude of the modes has been normalized so that the fundamental mode, $k = 1$, has unit amplitude. The magnitude of the superharmonic mode of the perturbation, $|a_1|$, is one tenth of the amplitude of the fundamental mode.

Figure 8 contains plots of the maximum growth rate versus the Floquet parameter for the perturbation for three values of the vorticity. These plots show that the vorticity effect is twofold: (i) the maximal growth rate increases as Ω decreases except for very long unstable perturbations, (ii) the bandwidth of unstable wavenumbers increases as Ω decreases. Note that these features were observed by Thomas *et al.* [21] and Francius and Kharif [22] within the framework of the nonlinear Schrödinger equation and the fully nonlinear Euler equations, respectively.

Hur and Johnson [11] found that small-amplitude, $2\pi/k$-periodic traveling-wave solutions of the Whitham equation are modulationally unstable if $kh > kh_{crit} \approx 1.146$. Later on, Hur and Johnson [14] found a formula for the boundary in the (Ω, k)-plane that separates stable and unstable small-amplitude, periodic, traveling-wave solutions to the vor-Whitham equation. A plot of this boundary is included in Figure 9. We numerically corroborated this

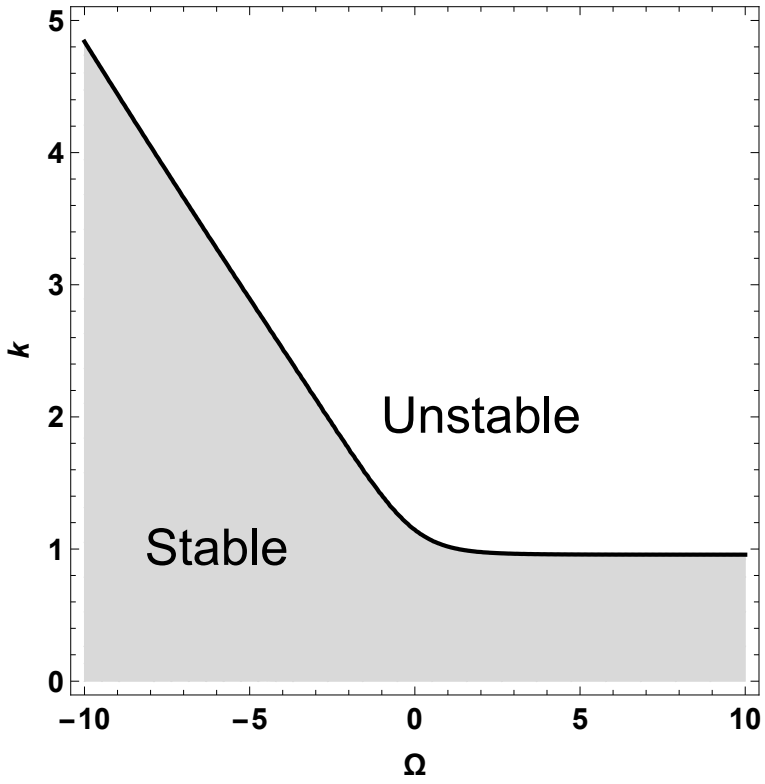

Figure 9: Stability diagram in the (Ω, k)-plane for small-amplitude, periodic, traveling-wave solutions to the vor-Whitham equation.

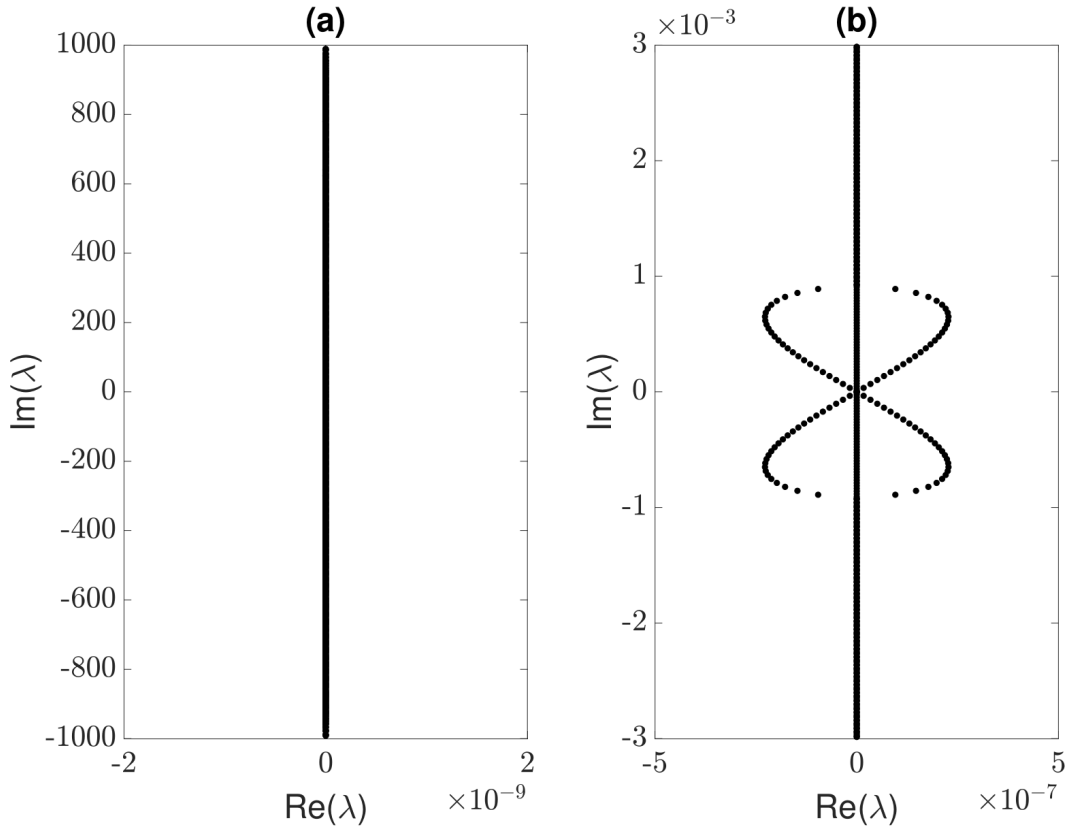

Figure 10: Stability spectra for (a) a small-amplitude solution to the vor-Whitham equation with $(\Omega, k) = (5, 0.9)$ and (b) a small-amplitude solution to the vor-Whitham equation with $(\Omega, k) = (5, 1)$. Note that the axes in the two plots are scaled differently. The spectrum in (a) lies purely on the imaginary axis and therefore the corresponding solution is spectrally stable. The spectrum in (b) has values with positive real parts and therefore the corresponding solution is unstable.

analytic result for a variety of Ω and k values. For example, we considered solutions just below and just above the critical value of $(\Omega, k) \approx (5, 0.96)$. We found that a small-amplitude (wave height of $4.3 * 10^{-3}$) solution to the vor-Whitham equation with $(\Omega, k) = (5, 0.9)$ is spectrally stable, see Figure 10(a) and that a small-amplitude (wave height of $3.3 * 10^{-3}$) solution with $(\Omega, k) = (5, 1)$ is unstable, see Figure 10(b). In summary, in the absence of vorticity we found a critical value in agreement with that of Hur and Johnson [11] and Sanford *et al.* [10] and in the presence of vorticity, we found critical values in agreement with the finding of Hur and Johnson [14]. The modulational instability of large-amplitude solutions in the presence of vorticity is a new finding.

4. Conclusion

The modulational instability of traveling-wave solutions of the Whitham equation in the presence of vorticity has been investigated numerically. The Whitham equation is an extension of the KdV equation which takes into account the full range of dispersion. We presented a sampling of our results which show the important qualitative results related to the modulational instability of periodic, traveling-wave solutions to the vor-Whitham equation. These results demonstrate that (i) the vorticity strongly modifies the growth rate of the modulational instability, (ii) a critical wave steepness above which the solutions become unstable exists whatever the value of the vorticity, and (iii) the critical depth under which the solutions restabilizes depends on the vorticity.

References

[1] McLean, J. Instabilities of finite-amplitude gravity waves on water of finite depth. *J. Fluid Mech.* **1982**, *114*, 331–341.

[2] Francius, M.; Kharif, C. Three-dimensional instabilities of periodic gravity waves in shallow water. *J. Fluid Mech.* **2006**, *561*, 417–437.

[3] Whitham, G. Linear and nonlinear waves. *John Wiley and Sons* **2017**.

[4] Carter, J.D. Bidirectional Whitham equations as models of waves on shallow water. *Wave Motion* **2018**, *82*, 51–61.

[5] Moldabayev, D.; Kalisch, H; Dutykh, D. The Whitham equation as a model for surface water waves. *Physica D* **2015**, *309*, 99–107.

[6] Klein, C.; Linares, F.; Pilod, D. ;Saut, J.C., On Whitham and related equations. *Studies in Applied Mathematics* **2018**, *140*, 133–177.

[7] Ehrnström, M.; Kalisch, H. Traveling waves for the Whitham equation. *Differential and Integral Eq.* **2009**, *22*, 1193–1210.

[8] Ehrnström, M.; Kalisch, H. Global bifurcation for the Whitham equation. *Math. Modeling Natural Phenomena* **2013**, *8*, 13–30.

[9] Kharif, C.; Abid, M. Nonlinear water waves in shallow water in the presence of constant vorticity: A Whitham approach. *Eur. J. Mech./B Fluids* **2018**, *72*, 12–22.

[10] Sanford, N.; Kodama, K.; Carter, J.; Kalisch, H. Stability of traveling wave solutions to the Whitham equation. *Phys. Lett. A* **2014**, *378*, 2100–2107.

[11] Hur, V.; Johnson, M. Modulational instability in the Whitham equation for water waves. *Studies Appl. Math.* **2014**, *134*, 120–143.

[12] Benjamin, T.; Feir, J. The disintegration of wave trains on deep water. Part 1. Theory. *J. Fluid Mech.* **1967**, *27 (3)*, 417–437.

[13] Whitham, G.B. Non-linear dispersion of water waves. *J. Fluid. Mech.* **1967**, *27*, 399–412.

[14] Hur, V.; Johnson, M. Modulational instability in the Whitham equation with surface tension and vorticity. *Nonlinear Analysis* **2015**, *129*, 104–118.

[15] Kharif, C.; Abid, M.; Touboul, J. Rogue waves in shallow water in the presence of a vertically sheared current. *J. Ocean Eng. and mar. Energy* **2017**, *3(4)*, 301–308.

[16] Hur, V. Shallow water wave models with constant vorticity. *Eur. J. Mech./B Fluids* **2017**, *10.1016*.

[17] Bjornestad, M.; Kalisch, H. Shallow water dynamics on linear shear and plane beaches. *Phys. Fluids* **2017**, *073602*.
g

[18] Deconinck, D.; Kutz, J.N. Computing spectra of linear operators using the Fourier-Floquet-Hill method. *J. Comp. Phys.* **2006**, *219*, 296-321.

[19] Johnson, M.A., 2013. Stability of small periodic waves in fractional KdV-type equations. *SIAM J. Math. Anal.* **2013**, *45*, 3168–3193.

[20] McLean, J.; Ma, Y.; Martin, D.; Saffman, P.; Yuen, H. Three-dimensional instability of finite amplitude water waves. *Phys. Rev. Lett.* **1981**, *46*, 817–820.

[21] Thomas, R.; Kharif, C.; Manna, M. A nonlinear Schrödinger equation for water waves on finite depth with constant vorticity. *Phys. Fluids* **2012**, 127102.

[22] Francius, M.; Kharif, C. Two-dimensional stability of finite-amplitude gravity waves on water of finite depth with constant vorticity. *J. Fluid Mech.* **2017**, *830*, 631–659.